ELSEVIER

Journal of Hazardous Materials 56 (1997) 315–332

JOURNAL OF HAZARDOUS MATERIALS

Ion velocity in soil solution during electrokinetic remediation

Fabienne Baraud *, Sylvaine Tellier, Michel Astruc

Laboratoire de Chimie Analytique, EP 132 CNRS, Université de Pau et des Pays de l'Adour, 64000 PAU, France

Received 6 January 1997; accepted 6 June 1997

Abstract

During the electrodecontamination of soils the pollutants' fluxes control the decontamination time. Application of this technique to real cases necessitates some simple predictive tools to rapidly evaluate the feasibility of the method. The pollutants' fluxes depend on their concentration and their velocity in the soil solution. In this paper our interest focuses on this pore velocity. A simple expression for the velocity of cationic species in the pore solution is proposed, for a wide range of situations where electroosmosis and electromigration are the major contributing ion transport mechanisms (governed by the electrical field applied). An adapted methodology is developed (pH control, steady-state conditions) and applied at laboratory scale using kaolinite as a soil model and some cations as model pollutants. Experimental results and theoretical calculations are compared. © 1997 Elsevier Science B.V.

Keywords: Electrokinetic remediation; Kaolinite; Velocity

1. Introduction

Soil contamination is becoming a key environmental issue, due to its importance in ecosystems, and the influence it has on the quality of ground water and food, placing human health at a risk [1].

Early remedial action—especially when metallic pollution was present—consisted of excavation and removal of the contaminated soil layers from the site and disposal in a landfill. In many cases, an in situ clean up process would have been immensely helpful, i.e., to avoid ground water contamination.

* Corresponding author. Tel.: +33 5 59 92 3090; fax: +33 5 59 02 9377; e-mail: lca@messv2.univ-pau.fr.

PII S0304-3894(97)00073-3

With more emphasis now placed on in situ technologies, the electrokinetic remediation process is emerging as one of the most promising. Major advantages of this method are: a possible utilisation in or ex situ; a low power consumption (low operation costs); a potential applicability to a wide range of contamination situations, as a number of studies, both in the field and at laboratory scale, have already been reported. It can be used to remove, ionic or non-ionic chemical species, heavy or light metals [2–6], as well as organic compounds [7–11].

The basic principle is simple: electrodes are inserted in the soil mass and a DC electrical field is applied. Due to different transport mechanisms, the polluting species are transported to the electrodes and may be removed from the soil.

The method, when applied at laboratory scale to real contaminated samples, gives promising results. These experiments also reveal the complexity of the overall phenomena that result when there are couplings between hydraulic, electrical, thermal and chemical driving forces and flows. A better understanding of these phenomena is necessary to get a theoretical modelling of the entire process, which will be immensely helpful to predict, optimise and adapt the method to each particular case. Then, prediction of the decontamination time is of great importance to estimate power consumption of such a process. This time is all the lower when the effective transport velocity of contaminants is high. But this decontamination velocity depends on two parameters.

First, the pollutant concentration in the soil solution, which is related to the various possible solid/liquid interactions (adsorption/desorption, complexation, precipitation, dissolution...) and to the speciation of the species of interest (i.e. ionic charge modification) also the ionic concentrations are then closely controlled by sorption and speciation phenomena.

Second, the velocity in the pore solution when species are actually in the soil solution and not engaged in any reaction or interaction. This velocity mainly depends on the different driving forces (electric potential gradient, hydraulic head difference, concentration gradient) and is not so closely related to soil properties, except for the electroosmosis phenomenon.

Various theoretical treatments incorporating electrical gradients are proposed [8,12,13]. A complete complex model of electrokinetic soil remediation first necessitates a simplified approach of ionic transport in the pore solution.

In a study of the feasibility of using electrical gradients to retard or stop the migration of contaminants, Yeung developed a one-dimensional model for the transport of pollutants through compacted clays. Based on the principles of irreversible thermodynamics, this theory describes the simultaneous flows of water, electricity and contaminant species that can occur during an electrokinetic process [13,14]. The coupling between electrical, hydraulic, thermal and chemical gradients is responsible for the different coupled or direct flows of water, electricity, heat, and ions, as indicated by Mitchell [15]. A direct flow is a flow of one type driven by its own potential gradient whereas a coupled flow is a flow of one type (hydraulic flow for example), driven by a potential gradient of another type (electrical potential gradient for example). This theory was developed for a system consisting of one anion and one cation in two compartments separated by a charged membrane. This treatment can be easily generalised to multicom-

ponent systems and to charged clays, clays being then assimilated to semi-permeable membranes [15,16].

In the present work, Yeung's complex theoretical analysis was used to elaborate a simplified one-dimensional model expressing the velocities of ions during the treatment process. Our purpose is to study an *electro*-decontamination (not electro-kinetic *barrier*). Then, we didn't study the influence of hydraulic gradients that can be sufficient in some cases, i.e., high permeable soils, to realise a simple pumping of the pollution. Diffusion is not included in this work either: comparing effective diffusion coefficient and electrical mobility of different species lead to the conclusion, for many soils, that diffusion is a minor contributing component to the total flux [17]. In such conditions, corresponding to many real situations, the ionic velocity in the pore solution is particularly related to the ionic properties in the electric field as well as to spatial soil characteristics (ionic mobility, porosity, tortuosity).

Simplifying conditions were assumed (i.e. electromigration and electroosmosis are supposed to be the only two electrokinetic phenomena involved during the application of the electric field) so that a simple expression of the velocities of ions in the pore solution was developed. Experimental conditions were designed so as to fit these restricting hypotheses, and laboratory experiments were run with kaolinite as a soil model, using a pore solution containing one cation as the contaminant species model. Experimental velocities were then compared to the theoretical values calculated using the simplified model.

2. Theoretical analysis

2.1. General theory

Three important electrokinetic processes are involved during electrokinetic remediation [4,18,19].

Electroosmosis is the coupled flow of volume and charge in a porous material upon application of electrical field. The Helmholtz–Smoluchowski theory has been widely used for the description of this phenomenon, even though other models sometimes better fit the situation [15]. Charge on the soil surface is fundamental to the transport by electroosmosis, as the electroosmotic flow results from the action of the electrical field on the charged double layer of the pore surface [8,19].

Chemical or physical adsorption and lattice imperfections are some of the numerous phenomena governing surface charge of soil particles when in contact with aqueous solutions [20].

Casagrande [21] proposed a useful simple relation to quantify electroosmosis:

$$Q_{\mathrm{eos}} = \frac{K_{\mathrm{e}}}{S} \nabla(-E) \tag{1}$$

where Q_{eos}: electroosmotic water flow rate; K_{e}: electroosmotic permeability coefficient; S: cross-sectional area; $\nabla(-E)$: electrical potential gradient.

Electrophoresis describes the movement of charged particles within the pore fluid [18]. It becomes significant only when surfactants are introduced in the processing fluid to form micelles with other species, or when the technique is used for remediation of slurries [17].

Electromigration is the movement of ionic species present in the pore fluid. This migration is mainly responsible for current conduction in a soil–water system [3]. The ion electromigration velocity, v_{em}, is directly proportional to the electrical field E:

$$\vec{v}_{em} = u \cdot \vec{E} \tag{2a}$$

or

$$v_{em} = \frac{z}{|z|} u \cdot \nabla(-E) \tag{2b}$$

with u: ionic electric mobility in solution and z: electric charge of the ion. Other chemical processes may also play an important role: ion exchange and sorption on the soil surface; chemical reactions (precipitation, dissolution, complexation); development of chemical/osmotic gradients resulting from the chemical or sorption reactions; electrochemical reactions at the electrodes: electrolysis of water is usually the dominant reaction [17], involving at the anode: $2H_2O \rightarrow 4H^+ + 4\bar{e} + O_{2(g)}$, at the cathode: $2H_2O + 2\bar{e} \rightarrow H_{2(g)} + 2OH^-$; development of pH gradients, resulting from the combination of the production of H^+ and OH^- by water electrolysis, and of the electromigration of these ions.

The development and the evaluation of the effects of pH gradients have been the object of a large number of studies [1,3,8] [18,22–24]. Models predicting the pH distribution during electrokinetic processing have also been elaborated on by some authors [8,25].

Any flux or flow, J_i, may be related to the gradients or the driving forces X_j by [13,14]:

$$J_i = \sum_{j=1}^{n} L_{ij} X_j \ (i = 1,2 \ldots n) \tag{3}$$

where the phenomenological coefficients L_{ij} are independent of the driving force.

The driving forces considered by Yeung are the hydraulic gradient $\nabla(-P)$, the electrical gradient $\nabla(-E)$ and the concentration dependent part of the chemical gradients of the cation and the anion, respectively, $\nabla(-\mu_c^c)$, $\nabla(-\mu_a^c)$.

These forces generate four fluxes:

J_v: volume flow rate of solution per unit area.

I: electrical current density.

J_a^d, J_c^d respectively, diffusional flow rate of the anion and the cation per unit area, relative to the flow of water.

The corresponding set of phenomenological expressions is given by Mitchell et al. [13] and Yeung [14].

The L_{ii} are the conductivity coefficients of the direct flow and the L_{ij} $(i \neq j)$ are the coupling coefficients. These phenomenological coefficients are not independent, as a result of Onsager's fundamental theorem of reciprocity: $L_{ij} = L_{ji}$, $(i, j = 1, 2, \ldots)$.

Yeung gives detailed expressions for the different phenomenological coefficients related to experimentally measurable parameters [14].

2.2. Simplified theory

In the study presented here, the only effective driving force is the electrical gradient $\nabla(-E)$. (Evidences allowing to neglect the effects of hydraulic gradient $[\nabla(-P)=0]$, and chemical gradient, $[\nabla(-\mu_c^c)=0$, and $\nabla(-\mu_a^c)=0]$ will be given later.)

Under these supplementary hypothesis, the set of phenomenological equations is reduced, and using the expressions given by Yeung for the phenomenological coefficients leads finally to:

$$J_v = (K_e/\theta)\nabla(-E) \tag{4a}$$

$$I = (\kappa/\theta)\nabla(-E) \tag{4b}$$

$$J_a^d = u_a^* C_a \nabla(-E) \tag{4c}$$

$$J_c^d = u_c^* C_c \nabla(-E) \tag{4d}$$

with, θ: porosity of the porous medium; κ: electrical conductivity; u_i^*: effective electrical mobility in the porous medium; C_i: concentration of ion i in the pore solution.

The diffusional flow of ion i is related to the absolute flow J_i by [14]:

$$J_i = J_i^d + \frac{C_i}{C_w} J_i \tag{5}$$

where C_w: concentration of water; J_w: absolute flux of water.

The absolute flow for ion i is then:

$$J_i = u_i^* C_i \nabla(-E) + (C_i K_e/\theta)\nabla(-E) \tag{6}$$

The first term is due to electromigration and the second one represents the contribution of electroosmosis.

But C_i is defined with respect to the total sample volume whereas the accessible experimental data, c_i, is related to the volume of the pore fluid. For saturated soils, the volume of fluid is equal to the void volume: $C_i = \theta c_i$ [26].Eq. (6) becomes then:

$$J_i = u_i^* \theta c_i \nabla(-E) + (\theta c_i K_e/\theta)\nabla(-E) \tag{7}$$

As the velocity V_i is defined by:

$$V_i = J_i/\theta S c_i, \tag{8}$$

V_i may be calculated as:

$$V_i = \left(u_i^* + \frac{K_e}{\theta}\right)\nabla(-E) \tag{9}$$

A similar formulation was obtained by Alshawabkeh and Acar [27]. According to this Eq. (9), only two electrokinetic phenomena are controlling cation transport under these restricted conditions: electromigration and electroosmosis. $u_i^* \nabla(-E)$ represents the electromigration velocity, depending directly on the considered cation. $K_e/\theta \cdot \nabla(-E)$ is the electroosmotic velocity, related to the volumic flow.

All these parameters can be obtained from the literature (u_i^*, K_e) or from experimental conditions ($\nabla(-E)$, θ, K_e). A theoretical evaluation of cationic velocities in these specified conditions may then be calculated with Eq. (9).

3. Experimental

Electrokinetic transport was studied using a one-dimensional model system designed in the laboratory to determine ion velocities. An experimental methodology had to be developed in order to respect the hypothesis, i.e., negligible influence of hydraulic and concentration gradients.

A pure clay was chosen as a simple model of soil of low permeability to reduce hydraulic gradient influence. Kaolinite was chosen because it is easy to work with [16], it is the least active clay of the minerals with a low colloidal activity [24] and a relatively high electroosmotic water-transport efficiency [8].

The test cell in which the experiments were conducted (Fig. 1) consists of an horizontal rectangular PVC cell (50 cm × 4 cm × 4 cm). The kaolinite sample (total length 42.5 cm), saturated with an aqueous solution containing one alkaline cation (species of low reactivity but easily exchangeable cations), and one anion, is confined in the central part of the cell, separated from the two end chambers by filters of polyamide fibers. One electrode (platinum wire) is located at each end of the sample, immersed in the solutions of the end chambers. A direct current (DC) power supply is used to provide either a constant voltage or a constant current source. Each end chamber is supplied with an appropriate solution by a peristaltic pump. Overflow systems allow one to collect the effluents (resulting from the different flows) in reservoirs at both ends of the cell. The continuous introduction of solution at the anode allows a permanent electroosmotic flow which avoids soil dewatering and the development of internal hydraulic pressures. Overflow systems at the cell end chambers suppress the external hydraulic gradient. Thus: $\nabla(-P) = 0$. The experiments are run at constant room temperature; the electrical

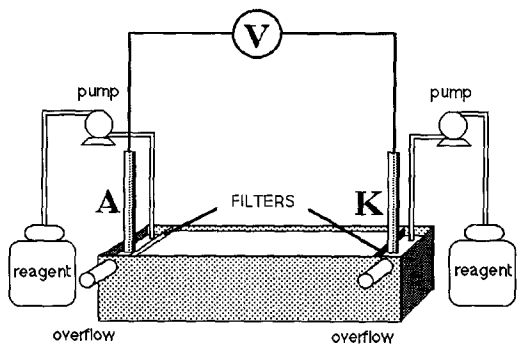

Fig. 1. Schema of laboratory test cell (A: anode, K: cathode, V: electric power supply).

intensity being low (inferior to 0.3 mA cm^{-2}), the Joule heating effect may be neglected. Therefore: $\nabla(-T) = 0$.

To impose the speciation conditions of the studied species and minimise possible interactions or reactions, a pH control was realised. Various options exist for controlling this parameter [1,5,19] [17]. Buffering compounds or reagents of controlled chemistry can be introduced in electrode chambers, and even move through the clay sample under the action of electrokinetic phenomena [19] [28,29].

The option chosen for this work was (as Jensen et al. in [30]) to supply an alkaline solution to the anodic compartment and an acidic solution to the cathodic compartment. Solutions of CH_3COO^- and of CH_3COOH (at the same concentration) were chosen respectively as alkaline and acidic solutions. An ethanoic buffer is thus produced in the cell. This buffer was chosen keeping in mind the application of the process to actual in situ situations, as it is a cheap, biodegradable and non toxic reagent.

Several advantages of this procedure can be outlined. The main one is that the presence of pH gradients through the cell resulting in a non-linear distribution of electrical gradients throughout the sample [2,23] is avoided. Due to this pH control, a regular electrical potential gradient is expected, as suggested by previous laboratory studies [31].

The results of five experiments are presented in this paper. The specified cations are: Na^+ (experiment number 1), K^+ (experiment numbers 2 and 3), Ca^{2+} (experiment numbers 4 and 5). Each cation was chosen so as to avoid any undesired chemical reaction (precipitation, complexation) in the working pH range (4–6), and to remain in solution as single ionic species.

Each experiment was run in two steps. (1) After preparation of the clay sample (kaolinite + ethanoate buffer solution), the experiment is initiated (under constant current or voltage) by introducing a continuous flow of a CH_3COONa solution at the anode and a CH_3COOH solution at the cathode, until steady state, to saturate the kaolinite with sodium ions. Na-kaolinite is then obtained. (2) In the second step sodium introduction at the anode is stopped and replaced by the cation (X^{n+}) of interest, in the form of ethanoate salt ($(CH_3COO)_nX$). In the early stages of this second part of the experiment, the exchange reaction Na^+/X^{n+} takes place. The experiment is run until steady state ion fluxes are obtained (i.e., stationary and equal inlet and outlet ion fluxes). By definition, there is no retardation of solute species under steady state conditions. These conditions guarantee that no chemical/electrochemical and no exchange/adsorption reactions are occurring in the sample anymore; therefore, concentration gradients are nil: $\nabla(-C_c^c) = 0$, and $\nabla(-C_a^c) = 0$. Supposing that our working concentrations are low enough to apply the laws governing dilute solutions, the relation $\nabla(-\mu_i) = (RT/C_i)\nabla(C_i)$ is verified leading to $\nabla(-\mu_c^c) = \nabla(-\mu_a^c) = 0$.

Experimental conditions are described below, except for experiment number 3. Sample preparation consists of mixing 500 g of kaolinite (extra pure, low bacteria content, MERCK) with 400 ml of ethanoate buffer solution, CH_3COONa/CH_3COOH, 10^{-2} mol l^{-1}.

During the whole experiment, a CH_3COOH solution, 10^{-2} mol l^{-1}, is continuously introduced in the cathodic compartment, with a 30 ml h^{-1} volumetric flow rate. At the anode, the 10^{-2} mol l^{-1} solution of CH_3COONa, introduced during the conditioning

step, is replaced by a solution of $(CH_3COO)_nX$, 10^{-2} mol l^{-1} in ethanoate ion (experiments 2 and 3: potassium ethanoate CH_3COOK; experiments 4 and 5: calcium ethanoate $(CH_3COO)_2Ca$).

The volumetric flow rate at the anode is the same as at the cathode.

The conditions of experiment number 3 are almost identical, except for the concentration values, which are all 10^{-1} mol l^{-1} instead of 10^{-2} mol l^{-1}.

Except for the last one, in which constant current conditions were imposed (4 mA corresponding to a current density of 0.28 mA cm^{-2}), the experiments were run under a constant voltage of 50 V across the test cell (a theoretical electrical potential gradient of 1 V cm^{-1} in the clay is expected).

During the experiment, the volumetric flow rates (cathodic and anodic) and the composition of solutions collected in the reservoirs are determined. Concentrations of Na^+ and K^+ in the solutions were determined with a CORNING flame photometer 410 and Ca^{2+} by atomic absorption spectrometry with a IL 451 flame spectrometer. By the measurements of the volumetric changes of infuents and effluents, electroosmotic and ionic flow rates can then be calculated. Measurements of electrical gradient, current density, and pH profile across the cell are also made.

Additionally, at the end of each run, the kaolinite sample is divided into 12 sections. Each section is centrifuged for about 15 min (4000 rpm). The supernatant, i.e., the pore solution, is analysed for the cation of interest. The remaining kaolinite is dried for 16 h in an oven at 105°C to determine, by weight comparison, the water content.

4. Results and discussion

4.1. Fundamental hypothesis

4.1.1. pH control

pH measurements were made by inserting a combination pH electrode directly into the kaolinite sample. A satisfying pH control was observed during the whole experiment, all along the clay sample (Fig. 2) and in each end compartment (Fig. 3). The pH values obtained (4.5–5.5) are close to the pKa value of ethanoic acid (4.8) in aqueous solution.

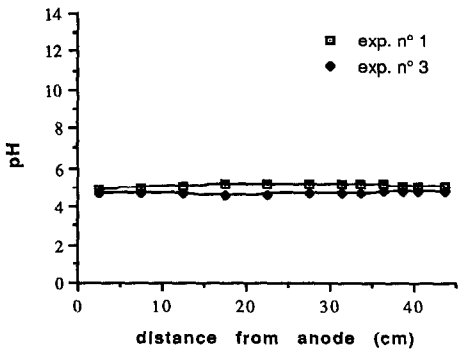

Fig. 2. pH across the kaolinite sample (experiment number 1: sodium, and number 3: potassium).

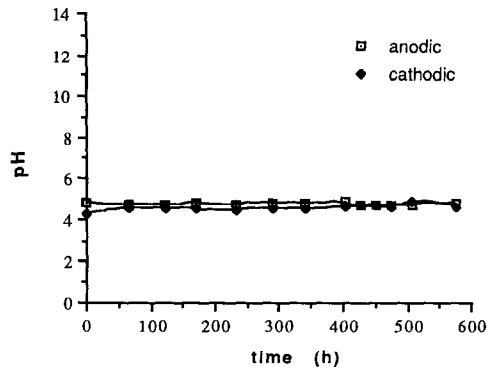

Fig. 3. Anodic and cathodic pH vs. time (experiment number 3: potassium).

4.1.2. Steady state

Steady state ion fluxes were obtained after various stabilisation periods. For the first part of the experiments, the stabilisation period is short, as the kaolinite has been pre-saturated with sodium ions during sample preparation. When a new cation X^{n+} is introduced in the anodic compartment and begins to migrate towards the cathode, the exchange reaction Na^+/X^{n+} occurs (Figs. 4 and 5), which generally delays the stabilisation period. Two effects have been noticed.

A concentration effect on K^+/Na^+ exchange: using 10^{-2} mol l^{-1} solutions, about 100 h were necessary in run number 2 to achieve complete exchange reaction (Fig. 4), whereas 55 h were sufficient at 10^{-1} mol l^{-1} in run number 3 (Fig. 5). This can be explained by two opposite effects. First, the potassium flux ratio is around 10 between run 2 and run 3. Inversely, a partial increase of the potassium retained is noticed in run 3, then corresponding to a partial increase of the available exchange sites. This could be probably correlated to a concentration effect on the double layer. But the rate of this

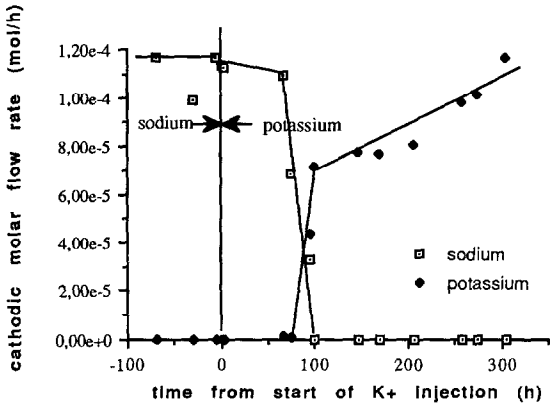

Fig. 4. Sodium and potassium exchange (experiment number 2).

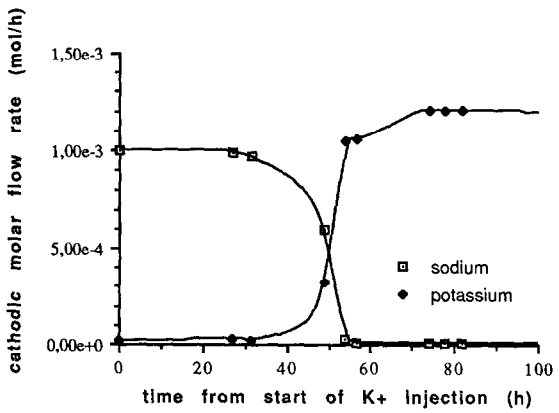

Fig. 5. Sodium and potassium exchange (experiment number 3).

increase is only around 3. Finally, more potassium ions are available proportionally to the exchange sites in run 3, which explains why the exchange period was shorter.

An effect of the electrical gradient on the Ca^{2+}/Na^{+} exchange: the exchange period necessitated 143 h in run number 4, but only 71 h in run number 5. During this transient period, the electrical potential gradient in run 5 was twice larger than in run 4, which affects the various fluxes, as shown previously in the theoretical development. In run 5, double values of the calcium fluxes were observed compared to run 4 during this period. Ca^{2+} ions could then reach more rapidly the exchange sites all across the sample, which shortened the exchange period if supposing that sorption reactions are fast and reversible.

At the end of the exchange period the steady state is obtained: as many cations are adsorbed as desorbed. On average, they stay in the soil solution and cross the cell without being influenced by any interaction. On Figs. 6 and 7, equal inlet and outlet flow rates of cations may be observed. This is obtained from the very beginning of the run for the sodium (Fig. 6), as Na^{+} is already present in the pore solution, introduced

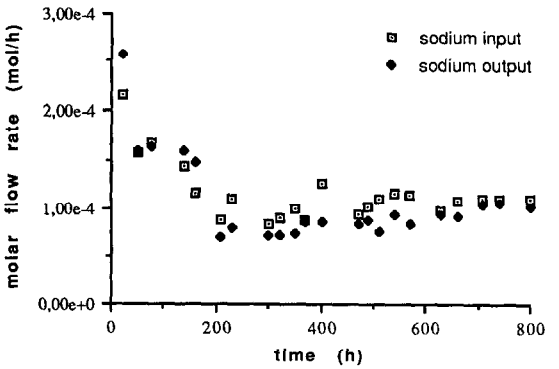

Fig. 6. Flow rates of sodium (experiment number 1).

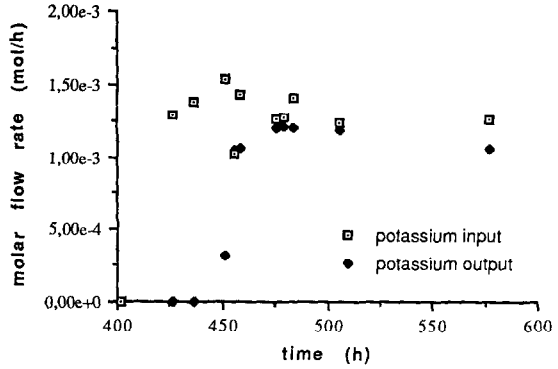

Fig. 7. Flow rates of potassium (experiment number 3).

during the sample preparation (pre-saturation). Inversely, a delay is first observed between input and output fluxes for the calcium (Fig. 7): it corresponds to the necessary time to cross and saturate the kaolinite.

The concentration profiles of cations in solution at the end of the run, as shown on Fig. 8, confirm that chemical gradients are negligible in our experimental conditions (diffusion evaluated in such conditions represents less than 1% of electrokinetic transport). A concentration effect is also reported on this figure: the final concentration ratio between runs 2 and 3 is the same than the initial one ($\approx 10\times$).

In these experimental conditions, pH is controlled, undesirable reactions are avoided, and sorption phenomena may be neglected when steady state is obtained. All hypotheses being satisfied it is possible to evaluate cation velocities.

4.2. Important parameters

4.2.1. Electroosmosis

The fluid is transported from the anode to the cathode, as the surface of kaolinite is negatively charged. The difference of introduced and collected volumetric flow rates

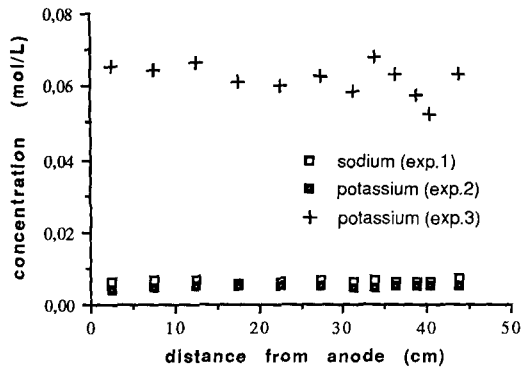

Fig. 8. Sodium or potassium in the pore solution (experiment number 1: sodium, and number 3: potassium).

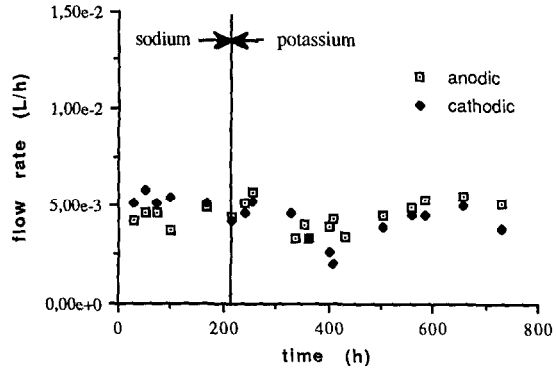

Fig. 9. Electroosmotic flow rate (experiment number 2: sodium/potassium).

(positive at the anode, negative at the cathode) corresponds to the electroosmotic flow rate (Q_{eos}). The positive difference between anodic and cathodic values probably results from uncontrolled evaporation.

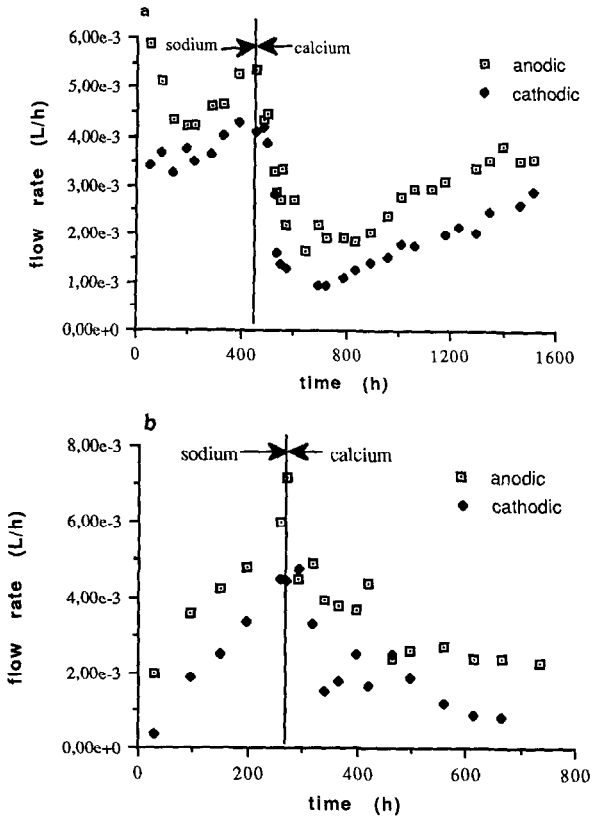

Fig. 10. (a) Electroosmotic flow rate (experiment number 4: sodium/calcium). (b) Electroosmotic flow rate (experiment number 5: sodium/calcium).

Table 1
Theoretical and experimental cationic velocities

Number of specified ion	[a]$u \cdot 10^5$ ($cm^2\ s^{-1}\ V^{-1}$)	$K^5_{e \cdot 10}$ ($cm^2\ s^{-1}\ V^{-1}$)	$\Delta V/\Delta x$ ($V\ cm^{-1}$)	Vtheo ($cm\ day^{-1}$)	V_{exp} ($cm\ day^{-1}$)
1 (Na^+)	51	10.0	0.72	35	36
2 (K^+)	67	7.3	1.04	59	63
3 (K^+)	67	6.4	1.12	51	48
4 (Ca^{2+})	57	7.2	0.54	30	31
5 (Ca^{2+})	54	2.8	0.60	25	25

[a]The ionic mobility u is given at run temperature.

It can be seen on Figs. 9 and 10a,b that the average electroosmotic flow rate is quite regular through each run, except for run numbers 4 and 5 (Fig. 10a,b): a net decrease of anodic and cathodic values is noticed when Ca^{2+} replaces Na^+. This can be attributed to the different valences of the ions, as related in the literature: decreasing flows are observed with increasing valence of the ions [32].

Using Casagrande's relation (Eq. (1)), the electroosmotic permeability coefficient, K_e, can be calculated for each experiment (reported in Table 1).

4.2.2. Electrical potential gradients

Steady electrical potential gradient profiles were obtained throughout the kaolinite sample and all along the experiments, when constant voltage was applied. No concentration effects are observed (Fig. 11a,b).

The resulting current density averages to 0.25 mA cm^{-2}, which is much less than the maximum values of 5 mA cm^{-2} suggested by Gray [29] and ensures negligible temperature effects [5].

Fig. 12 reports the last day profile of electrical potential gradients vs. distance from anode in experiments 4 and 5. Experiment number 5 was run under constant current conditions and the average potential gradient value is higher in this case (1.3 V cm^{-1} instead of 1 V cm^{-1} in experiments under constant voltage).

It should also be noticed that, especially in these last two experiments, an uncontrolled phenomenon occurs at the cathodic end of the kaolinite sample: a decrease of the measured electrical potential gradient in the vicinity of the cathodic solid/liquid interface has been observed (Fig. 12). This is correlated to an accumulation of calcium in this area (as molar fluxes are stationary and equal to the product of velocity by concentration, when electrical gradient and then velocity decreases, ionic concentration increases). No explanation can be given for the origin of this phenomenon in the present state of knowledge, but attention is hereby paid to the problem.

4.2.3. Cationic velocities

Experimental conditions are such that it is possible to apply Eq. (9). The theoretical velocity is obtained by using the data of the cationic region (i.e., output data). This calculated velocity is a mean value, representative of the effective ion transport; thus when the cation reaches the cathodic compartment, it has really crossed the whole kaolinite sample.

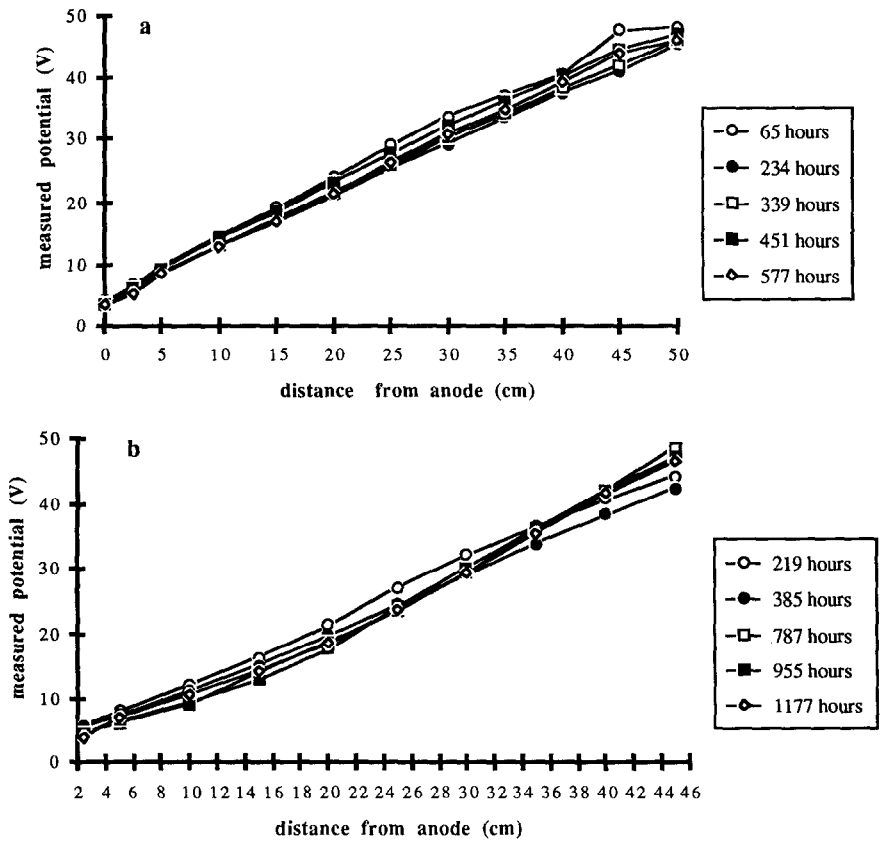

Fig. 11. (a) Electrical potential profile across the sample and throughout the run (experiment number 3: potassium). (b) Electrical potential profile across the sample and throughout the run (experiment number 4: calcium).

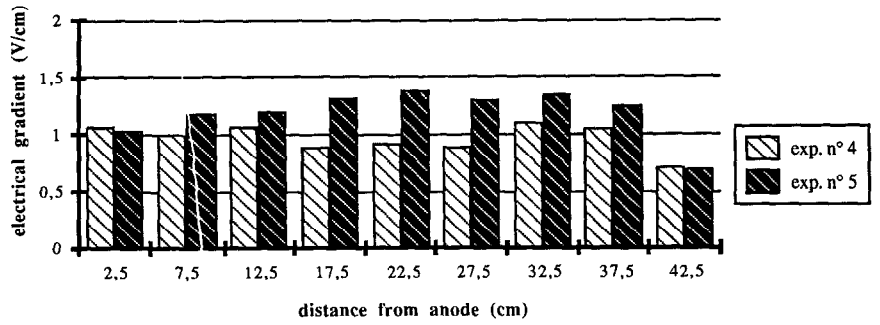

Fig. 12. Electrical gradients across the sample (experiment number 4 and number 5: calcium).

Then, the velocities are calculated from Eq. (9) with: K_e calculated from the cathodic evaluation of the electroosmotic flow rate; $\nabla(-E)$ obtained from the electrical potential difference between two points in the end section near the cathode (with V_{xi}, potential measured at the distance xi from the anode). Then: $\nabla(-E) = \nabla V/\nabla x = V_{x2}\text{-}V_{x1}/x2\text{-}x1$; the effective ionic mobility u^* is calculated from: $u = zDF/RT$ in the form $u^* = zD^*F/RT$, with: $D^* = D/\tau$, then: $u^* = u/\tau$ where D and D^* are respectively the diffusion coefficient of an ion in free solution and in a porous medium, z is the ionic charge, F the Faraday's constant, R the gas constant and T the absolute temperature. τ represents the tortuosity of the porous medium [26]. Shapiro and Probstein reported a value of $\tau = 1.24$ for the tortuosity of kaolinite [10]. Values of ionic mobilities in solution, u, are taken from the literature [33]. They are eventually adapted to the experimental temperature on the assumption of a 2% variation per °C [34].

The kaolinite being saturated in all experiments, the porosity is calculated by:

$$\theta = \text{fluid volume/total volume} \tag{10}$$

leading to $\theta = 0.672$.

The theoretical cationic velocity values obtained are compared in Table 1 to the experimental velocities, V_{exp}, evaluated from:

$$V_{exp} = J/\theta c \tag{11}$$

with, J: last day molar cationic flux; c: concentration in the pore volume of the cathodic end section.

A good agreement is obtained between experimental and theoretical results for the five experiments presented. Eq. (9) can actually predict cation velocities under the specified conditions.

Table 1 also presents experimental values of electroosmotic permeability and of electrical potential gradients of the cathodic end section. These velocities are of the same magnitude for the studied cations, as they get comparative electrical mobilities. The variations observed are related to the variations in experimental electroosmosis and electrical gradients. The relative part of electroosmosis varies between 9 and 25% of the total velocity. The actual influence of electroosmosis appears clearly by comparing experiments 4 and 5: with similar values of $\Delta V/\Delta x$, higher electroosmosis enhances calcium transport in run number 4, as shown by a higher experimental velocity (24% higher).

The comparison of run numbers 2 and 3 underlines the influence of the electrical potential gradient on the effective transport of potassium. As electroosmosis is quite similar in the two experiments a higher value of $\Delta V/\Delta x$ is correlated to an increased experimental velocity. The lowest values of velocities are obtained for the two runs with Ca^{2+} ions, corresponding, generally speaking, to the lowest electrical gradient for the five runs.

But this model can be generalised to the whole cell. For each of the 12 sections a theoretical value of velocity can be calculated, using the corresponding electrical gradient and an average value of electroosmosis ($\overline{Q_{eos}}$). Then, final concentrations can be evaluated for each section using Eq. (11), as the ionic flux J is supposed to be constant all along the sample (steady state conditions). The good agreement between experimen-

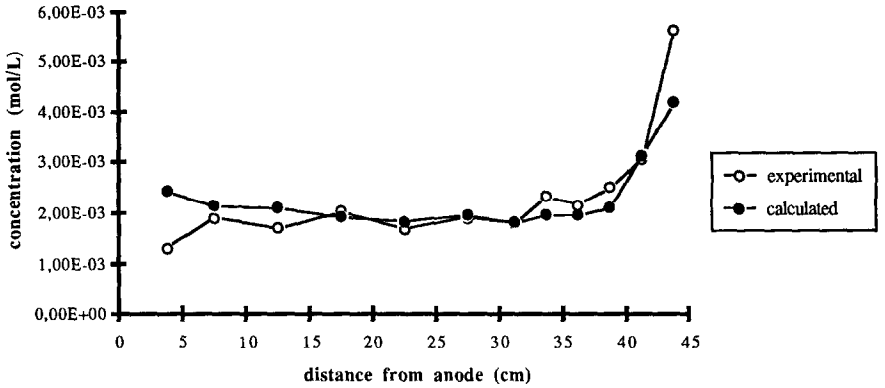

Fig. 13. Concentration profile of calcium across the sample (experiment number 5).

tal and calculated concentrations (Fig. 13) gives evidence that Eq. (9) is a good model for the whole sample. The difference noticed for the first and the last section is explained by the use of $(\overline{Q_{eos}})$ in the velocity calculation: due to the positive difference between anodic and cathodic electroosmosis, we get anodic $Q_{eos} > \overline{Q_{eos}} >$ cathodic Q_{eos}. It comes that with $\overline{Q_{eos}}$ the velocity in the first section is underestimated, so the concentration is overestimated as $C = J/\theta V$ (from equation (13)). Inversely, in the last section the concentration is underestimated. The use of an average value for the electroosmotic flow can be considered as a good approach giving satisfying results for the main part of the sample.

5. Summary and conclusion

A theoretical formalism based on the coupled flow theory [13,14] is presented, expressing cationic velocity in a porous medium submitted to electrical potential gradients. This method shows promise for the treatment of polluted soils, especially for cationic species such as metal ions, which are an important source of soil and water pollution: their removal efficiency is enhanced by the combined effect of the electroosmotic flow of water and of their electromigration transport, both of them being directed towards the cathodic compartment (at least, when the soil surface is negatively charged).

One-dimensional tests were designed using kaolinite as a soil model and one cation as a model contaminant. Good control of the phenomena occurring during the tests was achieved due to a careful choice of experimental methodology and the use of steady state conditions. Steady electrical potential gradients and constant pH values were maintained across the sample and throughout the run. Predictions of velocity values using the theoretical model compare very well with the results of the experiments. This velocity corresponds to the effective decontamination velocity of a cationic species that would not be involved in any reaction or interaction.

Several problems still have to be understood and solved to elaborate improved predictive models useful for actual application. First of all, a more detailed knowledge

of electroosmosis is needed to be able, for instance, to predict K_e value, and to explain the differences noted in quite similar experiments. However the simple Eq. (9) gives the average pore velocity of a cation that is on average not subject to any retardation phenomenon, via adapted methodology (steady state conditions). It's important to notice that under such conditions, the ion transport (then the treatment time) is mainly governed by the value of the electrical field applied. A different value for the effective decontamination velocity, compared to this theoretical velocity, indicates that electroosmosis and electromigration are not the only occurring mechanisms anymore: our model can already help to detect, study, and understand additional phenomena. As this equation is developed for experimental conditions of continuous circulating flows of reagents, it can eventually be used to model flow of purging and/or buffering solutions. That is of great importance since such methods can enhance the decontamination process. This expression (Eq. (9)), based on a validated theory, allows easy calculations that, when combined with some experimental investigations (to determine parameters like K_e value, tortuosity, porosity, concentrations) will help prospective users optimise the treatment conditions, i.e., to evaluate minimal time (and costs) required for a complete remediation of contaminated sites.

References

[1] R.E. Hicks, S. Tondorf, Environ. Sci. Technol. 28 (1994) 2203.
[2] J. Hamed, Y.B. Acar, R.J. Gale, J. Geotech. Eng. 117 (2) (1991) 241.
[3] S. Pamucku, J.K. Wittle, Environ. Prog. 11 (3) (1992) 241.
[4] S. Pamucku, J.K. Wittle, in: Proc. 14th Annual U.S. Department of Energy low-level Radioactive Waste Conference, 1993, pp. 256–278.
[5] B.E. Reed, M.T. Berg, J.C. Thompson, J.H. Hatfield, J. Environ. Eng. 121 (11) (1995) 805.
[6] L.I. Khan, M.S. Alam, J. Environ. Eng. 120 (6) (1994) .
[7] C.J. Bruell, B.A. Segall, M.T. Walsh, J. Environ. Eng. 118 (1) (1992) 68.
[8] A.P. Shapiro, P. Renauld, R. Probstein, Physicochem. Hydrodyn. 11 (5/6) (1989) 785.
[9] Y.B. Acar, R.J. Gale, US Patent 5 137 608 (1992).
[10] A.P. Shapiro, R. Probstein, Environ. Sci. Technol. 27 (2) (1993) 283.
[11] P.W. Sheridan, C.J. Athmer, M.A. Heitkamp, Environ. Sci. Technol. 29 (1995) 2528.
[12] Y.B. Acar, R.J. Gale, G.A. Putnam, J. Hamed, R. Wong, J. Environ. Sci. Health, Environ. Sci. Eng. 25 (6) (1990) 687.
[13] J.K. Mitchell, T.C. Yeung, Transportation Research Record 1288, (1991) 1.
[14] A.T. Yeung, J. Non-equilib. Thermodyn. 15 (1990) 247.
[15] J.K. Mitchell, Fundamentals of Soil Behaviour, Wiley, New York, 1984.
[16] H.W. Olsen, Am. Ass. Petrol. Geol. Bull. 56 (10) (1972) 2022.
[17] Y.B. Acar, A.N. Alshawabkeh, Environ. Sci. Technol. 27 (13) (1993) 2638.
[18] R. Lageman, W. Pool, G. Seffinga, Contaminated soil, Chem. Ind. (1989) 585.
[19] R. Probstein, R.E. Hicks, Science 260 (1993) 498.
[20] J.P. Legros, M. Chamayou, Les Bases Physiques Chimiques et Minéralogiques de la Science du Sol, Presses Universitaires de France (éditions), 1989.
[21] I.L. Casagrande, Géotechnique 1 (13) (1949) 159.
[22] R.E. Marks, Y.B. Acar, R.J. Gale, in: Proc. 47th Purdue Industrial Waste Conference, Lewis Publishers, Chelsea, MI, 1992, pp. 269–278.
[23] Y.B. Acar, J.T. Hamed, A.N. Alshawabkeh, R.J. Gale, Géotechnique 44 (2) (1994) 239.
[24] G.P. Korfiatis, L.N. Reddi, V. Montani, Transportation Research Record 1288, (1990) 35.

[25] A.N. Alshawabkeh, Y.B. Acar, J. Environ. Sci. Health A27 (7) (1992) 1835.
[26] C.D. Schackelford, J. Contam. Hydrol. 7 (1988) 177.
[27] A.N. Alshawabkeh, Y.B. Acar, J. Geotech. Eng. 122 (3) (1996) 186.
[28] R.F. Probstein, P.C. Renaud, A.P. Shapiro, US Patent 5 074 986 (1991).
[29] D.H. Gray, Géotechnique 20 (1) (1970) 81.
[30] J.B. Jensen, V. Kubes, M. Kubial, Environ. Tech. 15 (1994) 1077.
[31] M.C. Fourcade, Doctorat thesis, Pau, France (1996).
[32] M. Bonnemay, J. Royon, Techniques de l'ingénieur, (1974) D912-1.
[33] G. Milazzo, Electrochimie, Dunod, Paris, 1969.
[34] P. Gareil, Analysis 18 (1990) 221.